Morphological evolution of pulsed laser deposited ZrO_2 thin films

Cite as: J. Appl. Phys. **107**, 054311 (2010); https://doi.org/10.1063/1.3318604
Submitted: 27 May 2009 . Accepted: 19 January 2010 . Published Online: 08 March 2010

R. Álvarez, A. Palmero, L. O. Prieto-López, F. Yubero, J. Cotrino, W. de la Cruz, H. Rudolph, F. H. P. M. Habraken, and A. R. Gonzalez-Elipe

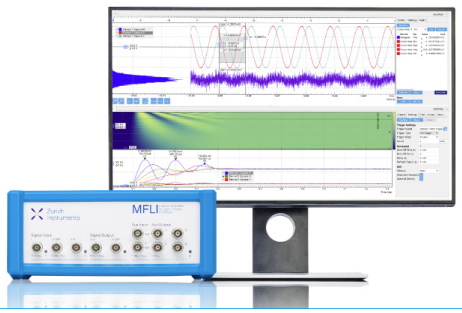

Morphological evolution of pulsed laser deposited ZrO_2 thin films

R. Álvarez,[1] A. Palmero,[1,a)] L. O. Prieto-López,[2] F. Yubero,[1] J. Cotrino,[1,3] W. de la Cruz,[2] H. Rudolph,[4] F. H. P. M. Habraken,[4] and A. R. Gonzalez-Elipe[1]
[1]*Instituto de Ciencia de Materiales de Sevilla, CSIC-Universidad de Sevilla, c/Americo Vespucio 49, 41092 Sevilla, Spain*
[2]*Centro de Nanociencias y Nanotecnología de la Universidad Nacional Autónoma de México, Km. 107 Carretera Tijuana-Ensenada, CP 22860 Ensenada, B.C. Mexico*
[3]*Departamento de Física Atómica, Molecular y Nuclear, Universidad de Sevilla, 41092 Sevilla, Spain*
[4]*Department of Physics and Astronomy, Surfaces, Interfaces, and Devices, Debye Institute, Utrecht University, P.O. Box 80.000, 3508 TA Utrecht, The Netherlands*

(Received 27 May 2009; accepted 19 January 2010; published online 8 March 2010)

Morphological evolution of ZrO_2 thin films deposited during pulsed laser deposition of Zr in O_2 atmosphere has been experimentally studied at two different film deposition temperatures, 300 and 873 K. The roughness exponent, α, the growth exponent, β, the coarsening exponent, $1/z$, and the exponent defining the evolution of the characteristic wavelength of the surface, p, for depositions at 300 K amounted to $\beta=1.0\pm0.1$, $\alpha=0.4\pm0.1$, $1/z=0.34\pm0.03$, and $p=0.49\pm0.03$, whereas for depositions carried out at 873 K amounted to $\beta=0.3\pm0.3$, $\alpha=0.4\pm0.2$, and $1/z=0.0\pm0.2$. Experimental error becomes important due to the flat morphology of the films inherent to the deposition technique. The change in the surface topography with the film temperature has been studied with the help of a simple Monte Carlo model which indicates the existence of two different growth regimes: a shadowing dominated growth, occurring at low temperatures, characterized by calculated values $\beta=1.00\pm0.04$, $\alpha=0.50\pm0.04$, $p=0.46\pm0.01$, and $1/z=0.35\pm0.02$ and a diffusion dominated growth that takes place at high temperatures as well as at low deposition rates, characterized by calculated values $\beta=0.15\pm0.08$, $\alpha=0.33\pm0.04$, and $1/z=0.33\pm0.07$. The good agreement obtained between the experimental and simulated parameters is discussed within the frame of the general characteristics of the deposition method. © *2010 American Institute of Physics*. [doi:10.1063/1.3318604]

I. INTRODUCTION

Pulsed laser deposition (PLD) has emerged as one of the simplest though most robust techniques to deposit a wide range of materials in the form of thin films. This success is due to the inherent versatility, flexibility, and high deposition rates that can be achieved in depositing thin films with controlled composition.[1–3] PLD is a physical vapor deposition process which, carried out under vacuum conditions, shares some characteristics with the molecular beam epitaxy and the sputter deposition methods. In the PLD technique, a laser illuminates a small spot, typically with an area less than 1 mm^2 on a solid target, which subsequently emits particles with a narrow emission angle. The emitted particles travel from the irradiated spot toward the deposition surface through a (reactive) gas, and are deposited on a substrate. Moreover, in PLD there is also a significant number of ions that reach the deposition surface with kinetic energies above the displacement energy threshold for bulk atoms in the material (typically around 100 eV), which results in the growth of compact thin film structures.[4] In this paper we study the growth of ZrO_2 thin films through the PLD technique and, in particular, the influence of the film temperature on the evolution of the surface morphology.

A key problem in the PLD technique relates to the understanding of the influence of energetic plasma particles, UV-light, high energy ion beam, etc. in the evolution of the film nanostructure in a far from equilibrium situation during growth.[1,5,6] From the point of view of the applications, surface morphology is quite relevant in order to optimize the electrical, optical, and heat conductivity properties of different materials in the form of thin films.[7] Among other theoretical approaches to understand the deposition process, kinetic Monte Carlo (MC) simulations represent a relevant tool to get important information about the thin film morphological evolution. According to Refs. 8–11 two important mechanisms must be taken into account: the shadowing of incident deposition particles, which becomes relevant when the incidence is nonperpendicular, and the diffusion mechanism, which takes into account the tendency of the material to relax into a more energetically stable structure. Besides, depending on the situation, other processes such as step-edge barriers, sputtering, etc. must also be taken into account.

The most common statistic used to describe the roughness of a surface is the standard deviation of the surface heights, $w(L,t)$, that depends on the lateral size of the surface, L, and time, t. Usually this quantity shows a power-law dependence on time during the first stages of growth, $w \sim t^{\beta}$, where β is known as the growth exponent. Furthermore, the lateral correlation lenght, ξ, that indicates the typical lateral length below which heights are statistically correlated, also follows a power-law in time as $\xi \sim t^{1/z}$, where $1/z$

a)Author to whom correspondence should be addressed. Electronic mail: alberto.palmero@icmse.csic.es.

is known as the coarsening exponent. Another important quantity is the so-called roughness exponent, α, linked to the self-affine scaling properties of the surface.[12] These three exponents, α, β, and z, are often related through the so-called Family–Vicsek dynamic scaling law,

$$w(L,t) = L^{\alpha} f(t^{\beta}/L^{\alpha}), \tag{1}$$

where $f(u)$ is a function with $f(u)_{u \ll 1} \sim u$ and $f(u)_{u \gg 1} \sim$ const. Thus, when $t \ll L^{\alpha/\beta}$ the surface roughness scales as $w(L, t \ll L^{\alpha/\beta}) \sim t^{\beta}$, and when $t \gg L^{\alpha/\beta}$ as $w(L, t \gg L^{\alpha/\beta}) \sim L^{\alpha}$, finding that the relation $z = \alpha/\beta$ holds.[12,13] Despite the fact that Eq. (1) has been found valid in many situations, mounded surfaces that exhibit wavelength selection often present a breakdown of this law due to the appearance of a second typical length, λ, linked with the typical distance between mounds on the surface. This quantity also follows a power-law in time, $\lambda \sim t^{p}$, and it has been recently demonstrated that when $p \neq 1/z$ the dynamic scaling relation, Eq. (1), does not hold anymore.[14]

The importance of experimentally achieving good control of surface properties of thin films deposited through the PLD technique, and the characterization of different growth regimes have motivated this paper, where we study the deposition of ZrO_2 thin films by PLD through the values of the exponents α, β, z, and p. For this, we have followed a combined approach. On one hand we have experimentally deposited ZrO_2 thin films for increasing deposition times at two different deposition temperatures, 300 and 873 K, and analyzed the surface roughness evolution. On the other hand, we have developed a simple MC model of the deposition, which includes the most relevant mechanisms during growth. From the comparison of experimental and simulated surface morphologies, the main features of the ZrO_2 growth at different temperatures are explained and discussed within the general characteristics of the PLD technique.

This paper is organized as follows: in Sec. II we describe the experimental setup and conditions used for the deposition of the ZrO_2 thin films, as well as the analysis of the surface topography and the calculation of the exponents α, β, z, and p. In Sec. III we explain the main characteristics of the MC model, whereas in Sec. IV we show the results of the model and discuss the experimental results in terms of the solutions. Finally in Sec. V we present the conclusions.

II. EXPERIMENTAL

A. Thin film preparation setup and conditions

Polycrystalline ZrO_2 thin films were grown with a commercial PLD setup (RIBER Co.). A zirconium target (99.8% purity) and a KrF excimer laser with $\lambda = 248$ nm, 20 ns pulse duration, and energy of 200 mJ per pulse, operated at 10 Hz were used to grow the films on a Si(111) wafer, which was placed in a substrate holder 10 cm away and in front of the target. The estimated energy density per pulse on the irradiated target surface was 0.3 J/cm^2. During the growth of ZrO_2 thin films, oxygen pressure in the deposition chamber was fixed at 0.6 Pa and the substrate temperature was varied between room temperature (300 K) and 873 K, for different samples series. These conditions imply a mean-free-path for the Zr atoms in the gas phase of few centimeters, so Zr particles arrive at the deposition surface after undergoing few collisions. However, Zr atoms require tens of collisions with the background gas particles in order to end up in thermal equilibrium.[15] Therefore, in our conditions, Zr particles arrive at the growth surface after experiencing some collisions, but still keeping an important directionality. Each series include films prepared during different deposition times: 250, 500, 1000, 2000, and 4000 s. The surface morphology was determined with a Nanotec Dulcinea atomic force microscope (AFM) using silicon tips of 10 nm radius in tapping mode.

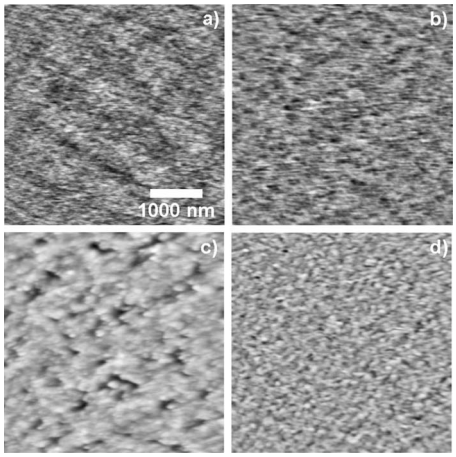

FIG. 1. Surface topology of the ZrO_2 thin films for different deposition times and temperatures obtained through AFM. (a) $t = 250$ s and $T_s = 300$ K, (b) $t = 250$ s and $T_s = 873$ K, (c) $t = 4000$ s and $T_s = 300$ K, and (d) $t = 4000$ s and $T_s = 873$ K.

B. Determination of the exponents of the ZrO_2 thin films

In Figs. 1(a)–1(d) we present the AFM measurements of the surface topography of the thin films for 250 and 4000 s deposition times and temperatures of 300 and 873 K. From the comparison between Figs. 1(a) and 1(c), as well as between Figs. 1(b) and 1(d), it seems clear that surface topography changes with time, involving the formation of mounds when the growth takes place at room temperature. Thus, it is apparent that temperature plays an important role in the evolution of the surface morphology. Using these measurements we have determined the exponents β, α, z, and p. The exponent β was calculated from the slope of the log-log representation of the surface roughness, w, as a function of time, whereas α was calculated through the height-height correlation function[12,13]

$$\zeta(r,t) = \langle [h(\vec{r}_1,t) - h(\vec{r}_2,t)]^2 \rangle_{|\vec{r}_1 - \vec{r}_2| = r},$$

where $h(\vec{r},t)$ is the height of the surface at a position given by $\vec{r}$ and time t, and $\langle \ldots \rangle$ refers to the average over all the possible values of $\vec{r}_1$ and $\vec{r}_2$ on the surface with $|\vec{r}_1 - \vec{r}_2| = r$. It is known that for distances above the lateral correlation length, i.e., at large values of r, the trend $\zeta \to 2w^2$ is found, whereas for values below (small values of r) $\zeta \sim r^{2\alpha}$.

In Fig. 2 we present the evolution of the film roughness with the deposition time for the growths at 300 and 873 K,

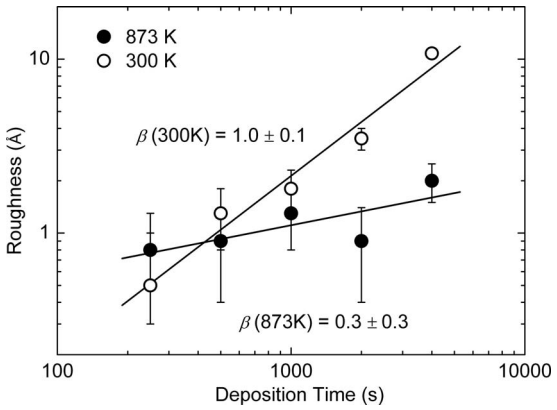

FIG. 2. Calculation of the exponent β for the films grown at 300 and 873 K.

used for the calculation of β. Films are clearly very flat with surface roughness below 1 nm in most of the cases, which is typical in PLD. Taking into consideration that AFM measurements include some noise due to the flatness of the samples, and that the measured surface roughness of the Si substrates amounts 0.5 Å, we find that most of the obtained topographies have high experimental error, especially the set deposited at 873 K as well as the first cases at 300 K. The flatness of the deposited films introduces some complexity in our analysis and represents one of the challenges in this paper. By fitting the roughness data in Fig. 2 we obtain that at room temperature the growth exponent amounts $\beta=1.0\pm0.1$, whereas at $T_s=873$ K we find the value of $\beta=0.3\pm0.3$. This difference between depositions at 300 and 873 K points toward the importance of thermally activated mechanisms inducing relaxation processes on the surface, thus changing the surface morphology.

Figure 3(a) shows the time evolution of the height-height correlation function of thin films grown at 300 K, with the corresponding value of ξ for each time, together with the height-height correlation function of the Si substrate. These graphs have been used for the evaluation of α, which is connected to the slope of the curve for small values of r. At a glance, it seems there is an upwards shift in the slope of the curves for increasing deposition times. This shift is connected to two possible causes: the first one is the existence of an anomalous scaling behavior.[16] This would imply the existence of local and nonlocal exponents, and a surface roughness evolution dependent on the measurement window size, l, and on time as $w(l,t)\sim t^{\beta}$ for $t\ll l^z$ and $w(l,t)\sim t^{\kappa}l^{\alpha_{loc}}$ for $t\gg l^z$, where α_{loc} is known as the local roughness exponent, and $\kappa=\beta-\alpha_{loc}/z$ (Refs. 17–19). This behavior has successfully explained the growth of films deposited by different deposition techniques (see for instance Refs. 20 and 21 and references therein). Conversely, the upwards shift in the slopes of the height-height correlation functions can be explained by considering the experimental inaccuracy of the AFM measurements found for deposition times $t=250$, 500, and 1000 s and the flatness of the films. From Fig. 3(a) it is clear that the height-height correlation function of the measured topography of the Si substrate possesses a similar slope for short distances as those obtained for deposition times $t=250$ and 500 s. This similarity indicates that most probably,

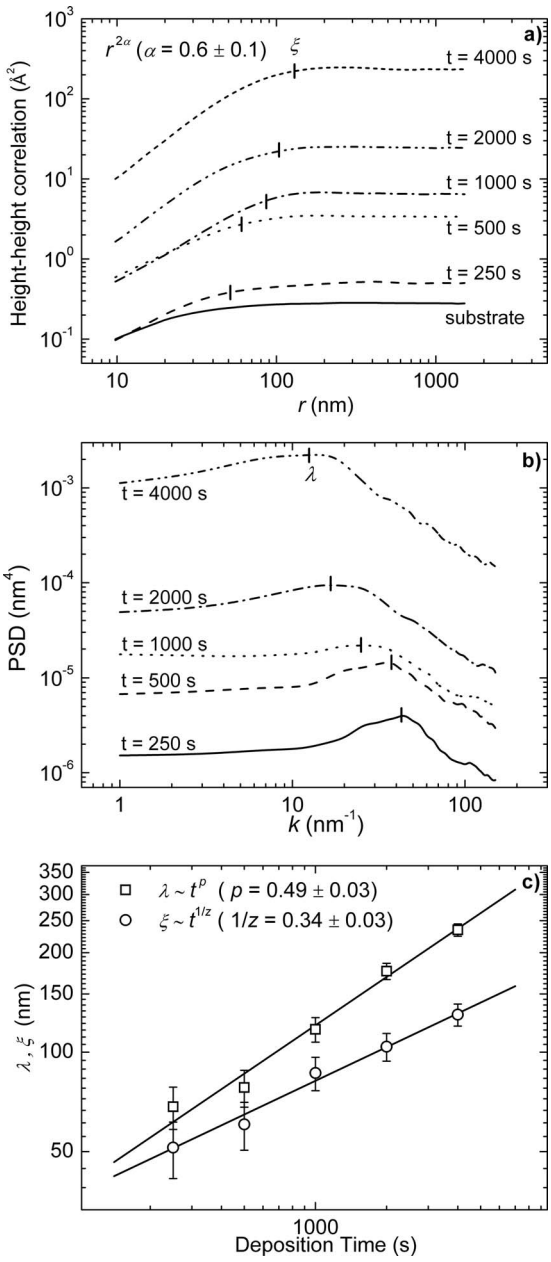

FIG. 3. Analysis of the surface topography for the films deposited at room temperature: (a) height-height correlation function, (b) power spectral density, and (c) correlation length and distance between mounds on the film surface as a function of the deposition time.

films grow so flat that surface correlations inherent to the substrate topography are still visible in the first stages of growth. In this way, the shift in the slope in Fig. 3(a) would correspond to a transition from a topography whose height correlations are dominated by the Si substrate to a topography whose correlations are defined by the film. This agrees with the fact that slopes for longer deposition times, $t=2000$ and 4000 s are the same. We think this second cause is most likely responsible for the changes in the slope present in Fig. 3(a), although we cannot rule out the existence of anomalous scaling due to the important noise of the measurements.

Taking into account the experimental error in Fig. 3(a), the roughness exponent of the film grown at 300 K is α

$=0.6\pm0.1$. However, we must introduce a correction factor due to the finite size of the AFM tip and its convolution with the surface topography. Aué and Hosson[22] studied this interaction and found that the value of α, when removing the tip influence, decreases by about a value of 0.2. Therefore, a more realistic value for α in our case is estimated to be $\alpha \simeq 0.4\pm0.1$. In Fig. 3(b) we show the power spectrum density (PSD) of the AFM topographies of the films grown at 300 K. Here it is clear the existence of a maximum for each deposition time, indicating the existence of wavelength selection on the surface. These maxima indicate the typical distance between mounds, λ.[12,13] In Fig. 3(c) we present the values of ξ and λ, found through Figs. 3(a) and 3(b), finding $p=0.49\pm0.03$ and $1/z=0.34\pm0.03$. In this way, the formation of mounds on the surface during growth introduces a new lateral scale length, implying a breakdown of the dynamic scaling law. Consequently, the relation $1/z=\beta/\alpha$ is not fulfilled for the studied growth, which becomes evident regarding the ratio between the calculated growth and roughness exponents. Interestingly, the measured value of p agrees well with the empirical trend $p\sim0.5$ found in the literature for a number of surfaces where wavelength selection takes place.[14]

As mentioned above, depositions carried out at $T_s=873$ K produce very flat, smooth, and unmounded surface morphologies. In Fig. 4(a) we present the height-height correlation function of these surfaces. There we notice that curves are not spatially ordered for increasing deposition times, which is coherent with the fluctuations of the surface roughness in Fig. 2, as each curve saturates at a value of $2w^2$, due to the noise introduced by the AFM measurements performed on such a flat samples. Consequently, quantitative results must be examined carefully before reaching any conclusion. A value of $\alpha=0.6\pm0.2$ is found, which taking into account the tip influence, leaves a value of $\alpha=0.4\pm0.2$.[22] From a qualitative point of view, films deposited at 873 K are much flatter than those deposited at room temperature, and show no mounds. This result becomes clear when seeing Fig. 4(b), where we depict the PSD graphs. These curves fall almost on top of each other, not showing maxima or any ordered pattern among them. In Fig. 4(c) we show the calculated values of ξ, which provide a value for the coarsening exponent of $1/z=0.0\pm0.2$. These results indicate that the noise introduced by the AFM measurements on such flat samples does not permit a clear quantitative analysis of the data.

Under the light of the results obtained for the samples deposited at 873 K it is clear that no quantitative information can be deduced when the film roughness is very low. This also applies to samples deposited at room temperature with low deposition time, where we have shown that features of the substrate topography are noticeable when performing the film surface analysis. However, due to the lack of accuracy of the AFM measurements for the high temperature set, it is not possible to conclude whether there is an anomalous scaling behavior in these cases or not.

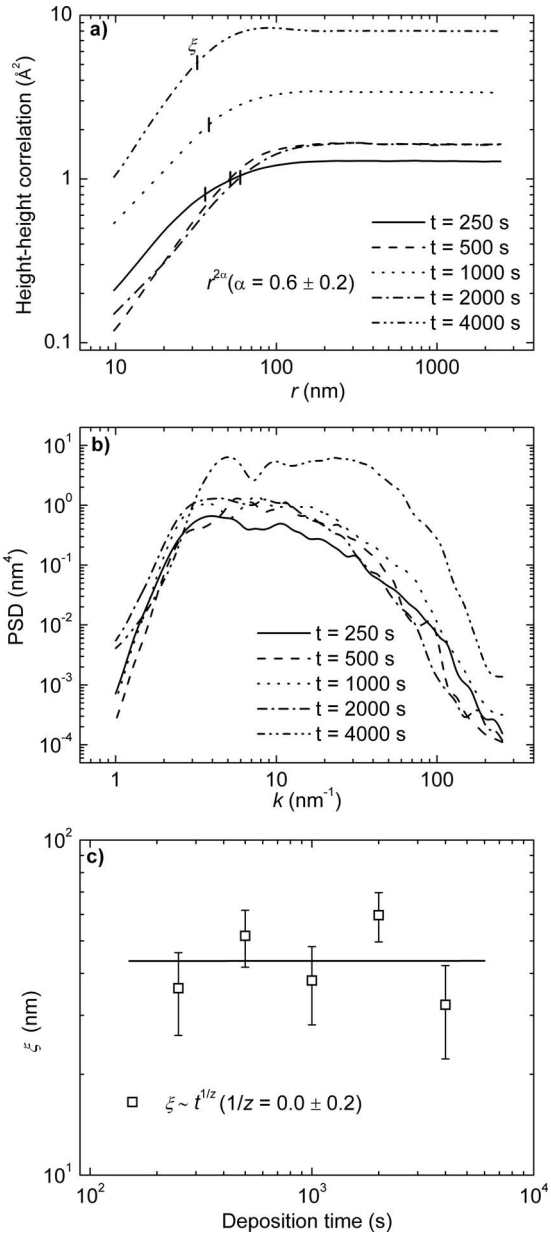

FIG. 4. Analysis of the surface topography for the films deposited at 873 K: (a) height-height correlation function, (b) power spectral density, and (c) correlation length as a function of the deposition time.

III. THEORETICAL MODEL

To explain the growth of the ZrO_2 thin films studied in this paper we have developed a MC model of the deposition. In our model we have followed an approach similar to that of Refs. 8–11, i.e., we consider the deposition of particles on a square two-dimensional $L\times L$ grid with periodic boundary conditions. Each deposited particle moves toward the substrate from an initial random position above the growth surface. For each particle, the direction of movement is defined by the spherical angles θ and φ, where $\theta\in[0,\pi/2)$ is the polar angle of incidence ($\theta=0$ is the direction normal to the substrate) and $\varphi\in[0,2\pi)$ is the azimuthal angle, which are randomly selected according to a given distribution function $I(\Omega)$, with $d\Omega=\sin\theta d\theta d\varphi$ being the differential solid angle. The movement of the particle continues until it hits the sur-

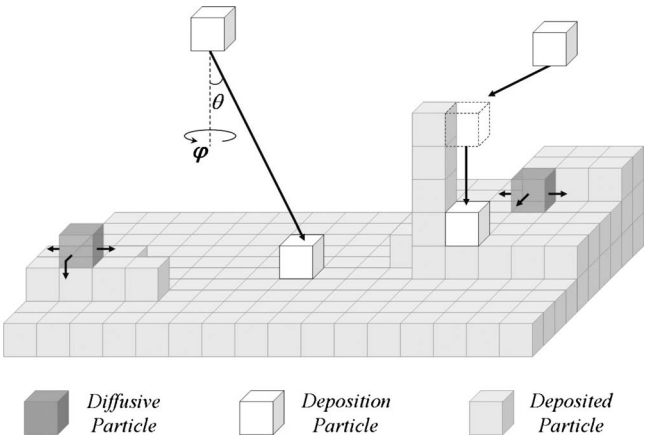

FIG. 5. Scheme with the main processes considered in the MC model.

face and it is deposited on the terrace below. This constraint is therefore typical of solid-on-solid models where surface height is univocally defined and where overhangs or voids are not allowed. This approximation is introduced in order to account for the high compactness of films deposited by PLD, and for the well-known important downhill current in the top layer when the deposition particles possess energies of few tens electron volt.[23] In this way, our model presents an important simplification of the surface kinetics of the film through the solid-on-solid approach, as will be discussed below. In addition, the ratio between the mean-free-path of the incoming particles and the characteristic length of the surface features is assumed to be large (Knudsen number $\gg 1$), and thus, collisions between deposition particles in their path toward the surface (in this scale range) are neglected in our description. In Fig. 5 we show a scheme of the elementary processes taken into account in our model.

The shape of $I(\Omega)$ represents an important issue in the model since the incorporation of Zr and O_2 particles into the film takes place through different mechanisms. For instance, high energy Zr particles reach the film with a very narrow angle distribution function, whereas oxygen in the gas phase follows a Maxwellian velocity distribution function. In our PLD system, the Zr deposition rate is typically below 10^{19} atoms s^{-1} m^{-2} whereas the number of oxygen molecules impinging on the surface can be estimated through the value of the average thermal velocity, which yields a value of approximately 10^{22} atoms s^{-1} m^{-2} under typical deposition conditions. This means that each deposited Zr atom encounters approximately 1000 oxygen molecules impinging on its neighborhood before another Zr atom is deposited. Thus, we approximate that each deposited Zr particle only bonds to O atoms on the surface and not to other Zr atoms. In this way, O atoms follow the distribution of Zr on the surface. This approximation is similar to that made in Ref. 24, where a MC model for the growth of $LaMnO_3$ thin films by PLD was developed, and where it was assumed that O atoms always follow the distribution of metallic atoms on the film surface. The angular distribution function followed by the deposition particles when arriving at the growth surface, $I(\Omega)$, is therefore related to the angular distribution function of the Zr atoms emitted from the target. If we consider both, the deposition surface and the emission spot in front of each other, the Zr atoms would arrive mostly perpendicularly, i.e., as a highly directed beam of particles. However, this beam of particles widens mainly due to two factors: the elastic scattering of the emitted particles on the background gas particles and the finite size effects of the emission region. In the model this widening is taken into account by writing $I(\Omega)$ as

$$dI(\Omega) \propto \exp(-\theta^2/2\sigma^2)d\Omega, \tag{2}$$

i.e., a Gaussian distribution function around $\theta=0$, with the parameter σ being a measure of the widening of the Zr beam when arriving at the substrate surface. Thus, our model permits to study qualitatively the effect of the widening of the particle beam through the quantity σ.

Thermally activated surface diffusion was taken into account in the model by introducing the parameter $\delta=D/F$, where D is the number of ad-particles on the surface that attempt to diffuse per unit time and F the number of deposited particles per unit time. Thus, δ provides the number of particles that attempt to diffuse on the surface per deposited particle. In our model we consider that after the deposition of each particle, δ randomly chosen particles from the surface attempt to diffuse and jump to a neighbor location. We consider the surface to be static during the diffusion of each particle, so the simultaneous movement of two or more particles on the surface is neglected. The jump probability is given by the Boltzmann factor $\exp(-E_D/k_BT_s)$, where E_D is the jump energy and k_B the Boltzmann constant. The value of E_D is obtained through the expression $E_D=E_0+n_cE_c+(\Delta E)\eta$, where E_0 is the jump energy related to the interaction with the terrace below, n_c is the number of next neighbors and E_c is the jump energy per neighbor. The factor $(\Delta E)\eta$ is introduced into the model as in Ref. 11. It represents a random term in the jump energy to take into account the energy variations per bond due to different local structures in the film. η is a random number between -1 and 1, and ΔE is the amplitude of the fluctuation, which is introduced in the model as an input parameter. Once the jump probability is calculated for a given particle, it is compared with a random number between 0 and 1. If this random number is lower than the jump probability, the jump is considered successful. In this way, any neighbor position at the same terrace height or below is considered available for the diffusive particle. Among these positions, we consider that the final destination of the particle is the one with the highest coordination number. Diffusion processes involving more than one jump per particle have been neglected in the model due to their low probability under the conditions of our experiment. Desorption has not been taken into account either, as the typical threshold energy for this process is several electron volts and it can be neglected under our experimental conditions. Other possible effects, such as step-edge barriers, re-emission, sputtering, or local reorganization of the film structure are discussed in Sec. IV.

IV. RESULTS OF THE MODEL AND DISCUSSION

Table I summarizes the values of the parameters used to solve the model. The values of E_0 and E_c were estimated in

TABLE I. Input quantities of the model and the values used to solve it.

Quantity	Values
E_0	0.1 eV
E_n	0.1 eV
ΔE	0, 0.1 eV
σ	$\pi/20$, $\pi/15$, $\pi/10$
T_s	300, 873 K
δ	0,1,2,...,40

such a way that E_D is within the same order of magnitude as other typical values for the jump energy found in literature.[25] Two values were considered for ΔE, 0 (no fluctuation) and 0.1 (the fluctuation amplitude is equal to E_c). For σ the three following values were considered: $\pi/20$, $\pi/15$, and $\pi/10$. These three values for σ allow us to study the influence of the broadening of $I(\Omega)$. Meanwhile, values between 0 and 40 have been explored for δ.

The simulated surfaces depict quite different aspects depending on the input parameters. Figures 6(a)–6(c) and 6(e) show the simulated surface morphology evolution for increasing thickness, $\sigma=\pi/15$ and $\delta=0$, i.e., when the diffusion is not introduced in the model. In this way, at initial stages of growth some small grains form on the film surface [Fig. 6(a)]. For increasing times we show that small mounds are formed due to the agglomeration and lateral growth of the original structures [Fig. 6(b)]. At higher deposition times, the mounds increase in size, whereas the valleys between them become relatively deeper [Figs. 6(c) and 6(e)].

In Figs. 6(d)–6(f) we show the simulated surface topographies for different values of σ, same mean height of the films and $\delta=0$. In these figures it is clear that the typical size of the mounds depends on the value of σ: the higher the value of σ, the larger the mounds and the deeper the valleys

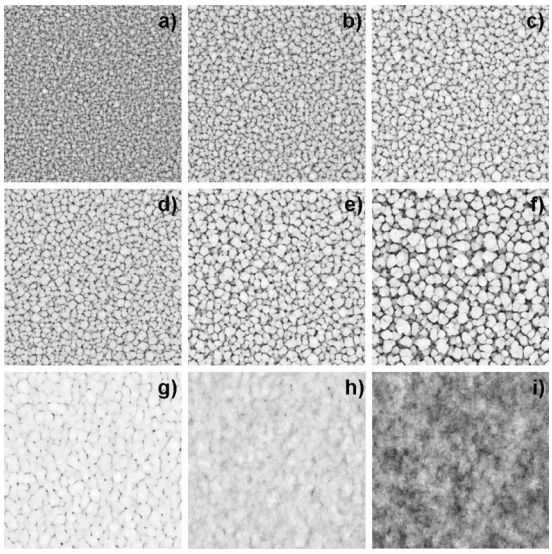

FIG. 6. Top view of the simulated surfaces for different values of the model input parameters. (a), (b), and (c) corresponds to $\sigma=\pi/15$ and $\delta=0$ for increasing film thicknesses, (d) $\sigma=\pi/20$ and $\delta=0$, (e) $\sigma=\pi/15$ and $\delta=0$, (f) $\sigma=\pi/10$ and $\delta=0$, (g) $\sigma=\pi/15$, $\delta=5$, $\Delta E=0$ eV, and $T_s=873$ K, (h) $\sigma=\pi/15$, $\delta=10$, $\Delta E=0$ eV, and $T_s=873$ K, and (i) $\sigma=\pi/15$, $\delta=20$, $\Delta E=0$ eV, and $T_s=873$ K.

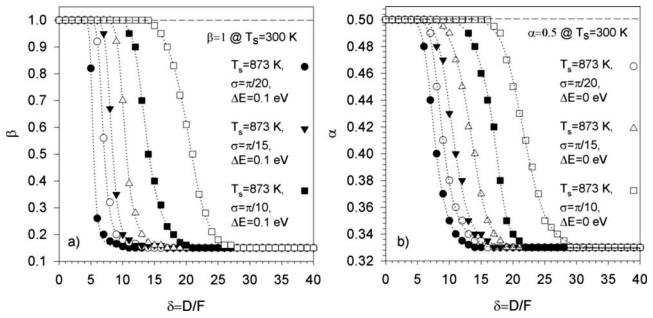

FIG. 7. Values of the exponents α and β obtained by the MC model for different values of the input parameters. (a) Growth exponent β and (b) roughness exponent α.

between them are. This result shows that there is a direct relation between the broadening of $I(\Omega)$ and the size of the mounds on the surface of the film, an effect that must be mediated by the shadowing mechanism on these surface structures, and that indicates the importance of the initial emission angle of the deposition particles and the subsequent scattering processes in the gas phase in the evolution of the thin film morphology.

In Figs. 6(g)–6(i) we study the influence of the diffusion mechanism on the simulated morphologies: in these cases we have taken the value $\sigma=\pi/15$ and depicted the solutions of the model for same height of the films and for different values of δ, keeping the rest of the input parameters constant. The selected values of δ, together with the case where $\delta=0$ in Fig. 6(e), were chosen to illustrate a transition from a shadowing dominated growth to a diffusion dominated growth (discussed in the next paragraph). Regarding Figs. 6(e) and 6(g)–6(i), it seems that diffusion flattens the surface of the film, and fills up the valleys on the surface, thus causing an important modification of the surface topography.

The changes observed in the surface morphology in Figs. 6(a)–6(i) can be related with different values of α, β, $1/z$, and p estimated from the calculated surface topographies. Figures 7(a) and 7(b) present the calculated values of α and β for the simulated growths at $T_s=873$ K and different values of σ, ΔE, and δ. In order to obtain these results, the model has been solved for $L=100$, 256, and 512, respectively, finding that the values of α and β are independent of the particular value of L and that there is no trace of anomalous scaling. In addition, to diminish the unavoidable statistical error on the MC simulations from one run of the model to another, we have carried out the simulation several times for each condition (i.e., for a given set of input parameters) and calculated the averaged values of the exponents and their dispersion, which has been considered the error. The first important feature in Figs. 7(a) and 7(b) is that the values $\beta=1.00\pm0.04$ and $\alpha=0.50\pm0.04$ are always obtained for $\delta=0$ and $\sigma>0$. This means that, despite the broadening of $I(\Omega)$, the growth is always dominated by the same mechanism (shadowing), which is responsible for the formation of mounds on the surface. For increasing values of δ three different regimes were found for all the studied cases at $T_s=873$ K.

- For low values of δ the exponents remain constant and

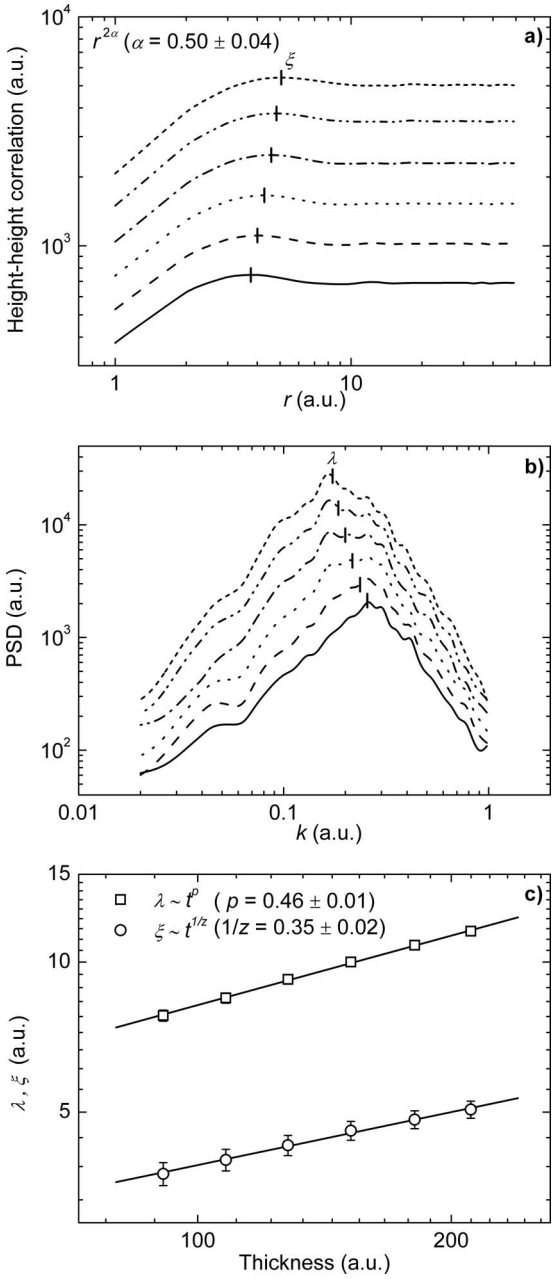

FIG. 8. Analysis of the surface topography for the simulated films when shadowing dominates the growth ($\sigma=\pi/15$ and $\delta=0$): (a) height-height correlation function, (b) power spectral density, and (c) correlation length and distance between mounds on the film surface as a function of the film thickness. In (a) and (b) upper curves correspond to thicker simulated films.

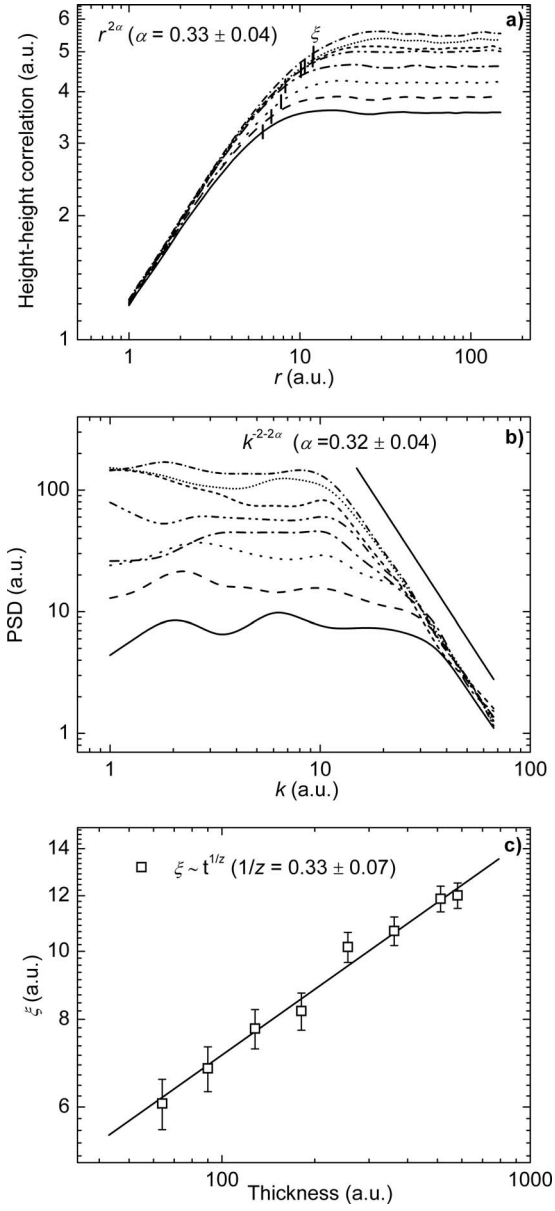

FIG. 9. Analysis of the surface topography for the simulated films when diffusion dominates the growth ($\sigma=\pi/15$, $\delta=20$, $\Delta E=0$ eV, and $T_s=873$ K): (a) height-height correlation function, (b) power spectral density, and (c) correlation length as a function of the film thickness. In (a) and (b) upper curves correspond to thicker simulated film.

equal to the values obtained without diffusion (i.e., for $\delta=0$): $\beta=1.00\pm0.04$ and $\alpha=0.50\pm0.04$. This first region thus corresponds to a shadowing dominated growth regime, with a typical morphology given by Fig. 6(e). In Figs. 8(a) and 8(b) we depict the height-height correlation function and the PSD curves for increasing thicknesses of the films. As expected, PSD curves show a clear peak, indicating the existence of a wavelength selection on the surface due to the appearance of mounds, and implying that the slopes of the curves are not related with the value of α. In Fig. 8(c) we show the results of the lateral coarsening study for the shadowing dominated region of the model, obtaining the values $p=0.46\pm0.01$ and $1/z=0.35\pm0.02$. The discrepancy between these two exponents indicates the breakdown of the dynamic scaling law in this region.

- For high values of δ, the exponents drop to $\beta=0.15\pm0.08$ and $\alpha=0.33\pm0.04$ no matter the value of ΔE or σ. This indicates that, in this regime, the growth is no longer dominated by the shadowing mechanism but by the thermally activated diffusion mechanism. Typical aspect of this surface morphology is given in Fig. 6(i). Figures 9(a) and 9(b) depict the height-height correlation function of the simulated growths and the PSD curves for different film thicknesses. The absence of clear peaks in these distributions shows that the surfaces are not mounded, so the

effect of shadowing has been minimized by thermal diffusion. In these conditions, dynamic scaling can apply to the surface growth, with the tail of the PSD decreasing as $k^{-2-2\alpha}$, being k the wave-number. The value of α obtained through Fig. 9(b) agrees quite well with the value found using the height-height correlation function [Fig. 9(a)], with $\alpha_{PSD}=0.32\pm0.04$. By studying the power dependence of ξ [calculated in Fig. 9(a)] on the deposition thickness, we have calculated the value of $1/z$ in the diffusion dominated region, finding $1/z=0.33\pm0.07$, which falls within the error range of the calculated value of β/α, and agrees with the fact that the dynamic scaling law applies in this region.

- For intermediate values of δ we find a transition interval between the shadowing dominated and the diffusion dominated regions [also depicted in Figs. 6(g)–6(i)]. Here, for increasing values of δ, the exponent β decreases, whereas α starts to fall for slightly higher values of δ. The particular value of δ that defines this region is determined by several factors such as, (i) the efficiency of the diffusion process (i.e., the value of the jump probability) and (ii) the depth of the valleys separating the mounds on the surface of the film. The former factor takes into account the influence of T_s and ΔE in the jump probability, whereas the latter accounts for the influence of the mound size, which depends on the value of σ. Thus, the competition between shadowing and diffusion determines the appearance of this region through the actual values of σ, T_s, and ΔE.

The three aforementioned regions for increasing values of δ are obtained for $T_s=873$ K, and this agrees with the results obtained in Ref. 10, where three regimes similar to those determined here were also found for sputtering deposition. For simulations at $T_s=300$ K, we have achieved different results: in this case the jump probability becomes so low that the shadowing mechanism dominates the growth regime no matter the value of δ, thus finding the exponents $\beta=1.00\pm0.04$, $\alpha=0.50\pm0.04$, $p=0.46\pm0.01$, and $1/z=0.35\pm0.02$ in all simulated conditions.

By considering the solutions of the model, it is possible to explain the experimental results obtained for the ZrO_2 thin films deposited through the PLD technique. We have found a transition from $T_s=300$ K, where the growth is characterized by measured exponents $\beta=1.0\pm0.1$, $\alpha=0.4\pm0.1$, $p=0.49\pm0.03$, and $1/z=0.34\pm0.03$ to another type of growth at $T_s=873$ K, where a flatter surface morphology is found, with exponents $\beta=0.3\pm0.3$, $\alpha=0.4\pm0.2$, and $1/z=0.0\pm0.2$. This is explained by considering a transition between a shadowing dominated and a diffusion dominated growths, attributed to the increase in the deposition temperature. In this way, the theoretical values obtained by the MC model compare quite well with the experimental ones: for a shadowing dominated growth, the values $\beta=1.00\pm0.04$, $\alpha=0.50\pm0.04$, $p=0.46\pm0.01$, and $1/z=0.35\pm0.02$ have been calculated in good agreement with the experimental results at 300 K, implying a breakdown of the dynamic scaling law. Meanwhile, for the diffusion dominated regime, values of $\beta=0.15\pm0.08$, $\alpha=0.33\pm0.04$, and $1/z=0.33\pm0.07$ have been obtained, which considering the important error due to the flatness of the films, agrees with the experimental results at 873 K. Furthermore, it is apparent that the surface morphologies evolution depicted in Figs. 6(a)–6(c) and 6(e) (corresponding to a shadowing dominated growth) are similar to the transition found between Figs. 1(a) and 1(c), whereas the case presented in Fig. 6(i) (corresponding to a diffusion dominated growth) possesses many similarities with the surface morphology in Figs. 1(b) and 1(d), and explains why all the depositions carried out at 873 K produce extremely flat morphologies. Our model calculations also show that a broader incident angle distribution function of the deposition species produces wider surface mounds: this effect is expected to gain relevance for higher residual pressures in the deposition chamber and for longer distances between the target and the substrate (higher values of σ) in any PLD process.

Our model also explains to some extent other results in the literature, e.g., those in Ref. 26 for the PLD deposition of ZnO thin films. There, the authors found two different stages during growth: a first stage where the material was mainly amorphous and defined by $\alpha=0.33\pm0.05$ and $\beta=1.0\pm0.1$ and a second stage in which the material was crystalline depicting pyramid-like structures on the surface with $\alpha=0.43\pm0.08$ and $\beta=0.60\pm0.01$. According to the results of our model, the experimental values of α and β obtained for the first stage of growth match quite well with our simulations for a shadowing dominated growth. However, our model is not able to explain satisfactorily the second stage. According to Ref. 26, crystallization involves the appearance of step-edge barriers during the film growth, a factor that seems responsible for the pyramidal structures developed on the surface and affects the surface mobility. Step-edge barriers are not introduced in our model which, consequently, will not be able to describe the evolution of the surface morphology of films where the crystallization process leads to the development of large crystal planes. Furthermore, exponents calculated using the theoretical model in the region where shadowing dominates the growth also matches quite well with those appearing in Refs. 10 and 14 for magnetron sputtering without re-emission. In those references, the function $I(\Omega)$ was taken as $dI(\Omega)\propto\cos\theta\, d\Omega$, i.e., an incident angle distribution function that can be easily reproduced with a low error by Eq. (2) in the range $\theta\in[0,\pi/2)$. Since the obtained exponents were independent of the particular value of σ in our model, it is expected that we find the same values when the shadowing mechanism dominates the growth. On the other hand, the diffusion dominated region in our model does not match with those presented in Ref. 10, where growths at low temperatures (about 350 K) were studied as a function of δ. As we saw before, low temperatures make the jump probability very low so diffusion is much less effective than in our case, with a temperature about 870 K, so different results are expected. Moreover, in the diffusion dominated regime our model obtains exponents close to those found by the

nonlinear conservative dynamics and nonconservative noise continuum model for 2+1 dimensional growths, that finds $\alpha=0.33$, $\beta=0.09$, and $1/z=0.27$.[12]

It is remarkable that a model developed to study the surface evolution of films grown by PLD reproduces results from magnetron sputtering depositions. Indeed the solid-on-solid approach is just a way to take into account the fact that the material tends to grow without overhangs and voids. Of course this approximation represents a simple way to study fundamental phenomena regarding the interaction between the deposition particles and the film, as well as the energy dependence of such interaction. Main differences between magnetron sputtering depositions and PLD, apart from the angular incidence of the particles, resides in the typical energy of the deposition particles [about 15–20 eV for magnetron sputtering depositions and ~100 eV for PLD (Ref. 27)] as well as the ion bombardment of the films during growth. As stated in Ref. 23, deposition of particles with incident kinetic energy of few tens electron volts causes a downhill current of particles in the top layer, producing an ultrasmoothening of the film surface. This effect must be present in both deposition techniques, though it is likely more effective in PLD due to the higher energy of the particles. It is not the goal of this paper to discuss the growth of films deposited by magnetron sputtering, but it seems that ion bombardment might play an important role in some conditions, so films grow compact. In magnetron sputtering, positive ions may impinge the film with energy of about 1–10 eV in dc discharges or 30–40 eV in rf discharges, whereas negative ions produced at the cathode sheath may reach the film with few hundreds electron volt. In each case, different downhill currents will be produced and hence different compactness of the films (even there is evidence of crystallization of films due to the high energy of negative ion bombardment[28]). These processes are treated in our model through a solid-on-solid approach, but this indeed is a first approach toward an energy dependent study of thin film growth. In Ref. 9 the energy dependence of the interaction between the deposited particle and the film surface was treated by introducing a sticking probability below unity and assuming an elastic re-emission of the deposition particle in case it does not stick, so it bounces off until it is deposited. Despite the fact that this model has obtained very interesting and promising results, the lack of experimental data about first and higher order sticking coefficients in our conditions, as well as a reliable scattering emission angle study of an incoming particle on a film surface, have made us decide for the simplest approach with lower number of unknown input parameters, i.e., sticking probability equals unity, no re-emission process, and a solid-on-solid simulation, which overall seems enough to reproduce the main characteristics of ZrO_2 thin films deposited by PLD.

V. CONCLUSIONS

In this paper we have studied the growth of ZrO_2 thin films deposited by PLD at two different growth temperatures, 300 and 873 K. We have determined the exponents that characterizes the growth and found that $\beta(300\ \mathrm{K})=1.0\pm0.1$, $\alpha(300\ \mathrm{K})=0.4\pm0.1$, $p(300\ \mathrm{K})=0.49\pm0.03$, and $1/z(300\ \mathrm{K})=0.34\pm0.03$, whereas for depositions carried out at 873 K surfaces are smoother and with a roughness in the order of magnitude of the experimental error of the measurements with exponents $\beta(873\ \mathrm{K})=0.3\pm0.3$, $\alpha(873\ \mathrm{K})=0.4\pm0.2$, and $1/z(873\ \mathrm{K})=0.0\pm0.2$. This change in the surface topography with the film temperature has been explained using a MC simulation of the growth process under the assumption of a solid-on-solid model where nonlocal shadowing and surface diffusion mechanisms compete to govern the development of the surface morphology. By considering the model calculations, it has been possible to explain the strong dependence of α, β, p, and $1/z$ on the film temperature by considering a transition between a shadowing dominated growth at 300 K and a surface diffusion dominated growth at 873 K. Despite the fact that this MC model represents a simplified description of the actual deposition of thin films through PLD, our model provides relevant information on the film growth, and can be applied to understand the main features of the surface morphology and roughness evolution of the analyzed ZrO_2 thin films and other similar results from literature.

ACKNOWLEDGMENTS

One of the authors (R. Álvarez) would like to acknowledge the JAE program of the Spanish Council of Research (CSIC). Another author (L.O. Prieto-López) would like to acknowledge CONACyT for M.Sc. scholarship. This work was partially supported by the projects PAPIIT (IN107808) and CONACyT (50203-F). Financial support by the Spanish Ministry of Innovation (Project Nos. MAT 2007-65764, PIE 200960I132, and the CONSOLIDER INGENIO 2010-CSD2008-00023) and the Junta de Andalucía (Project Nos TEP2275 and P07-FQM-03298) is also acknowledged. The authors also acknowledge to J. A. Diaz, E. Aparicio, I. Gradilla, J. Peralta, P. Casillas, D. Dominguez, and V. García for their technical support.

[1] M. Ohring, *Material Science of Thin Films, Materials and Structure*, 2nd ed. (Academic Press, New York, 2002).
[2] W. de la Cruz, G. Soto, and F. Yubero, Opt. Mater. **25**, 39 (2004).
[3] L. O. Prieto-López, F. Yubero, R. Machorro, and W. De La Cruz, Microelectron. J. **39**, 1371 (2008).
[4] H. U. Krebs, in *Pulsed Laser Deposition of Thin Films*, edited by R. Eason (Wiley Interscience, New York, 2007), Chap. 16, p. 363.
[5] I. Denysenko, K. Ostrikov, M. Y. Yu, and N. A. Azarenkov, J. Appl. Phys. **102**, 074308 (2007).
[6] E. Tam, I. Levchenko, K. Ostrikov, M. Keidar, and S. Xu, Phys. Plasmas **14**, 033503 (2007).
[7] M. V. Ganduglia-Pirovano, A. Hofmann, and J. Sauer, Surf. Sci. Rep. **62**, 219 (2007).
[8] T. Karabacak, G.-C. Wang, and T. M. Lu, J. Appl. Phys. **94**, 7723 (2003).
[9] T. Karabacak, Y.-P. Zhao, G.-C. Wang, and T.-M. Lu, Phys. Rev. B **66**, 075329 (2002).
[10] T. Karabacak, Y.-P. Zhao, G.-C. Wang, and T.-M. Lu, Phys. Rev. B **64**, 085323 (2001).
[11] F. Elsholz, E. Schöll, and A. Rosenfeld, Appl. Phys. Lett. **84**, 4167 (2004).
[12] A. L. Barabàsi and H. E. Stanley, *Fractal Concepts in Surface Growth* (Cambridge University Press, Cambridge, England, 1995).
[13] M. Pelliccione and T.-M. Lu, *Evolution of Thin Film Morphology* (Springer-Verlag, Berlin, 2008).
[14] M. Pelliccione, T. Karabacak, C. Gaire, G.-C. Wang, and T.-M. Lu, Phys. Rev. B **74**, 125420 (2006).
[15] A. Palmero, H. Rudolph, and F. H. P. M. Habraken, J. Appl. Phys. **101**,

083307 (2007).
[16]A. Yanguas-Gil, J. Cotrino, A. Barranco, and A. R. Gonzalez-Elipe, Phys. Rev. Lett. **96**, 236101 (2006).
[17]J. M. Lopez, M. A. Rodriguez, and R. Cuerno, Physica A **246**, 329 (1997).
[18]J. M. López, M. A. Rodríguez, and R. Cuerno, Phys. Rev. E **56**, 3993 (1997).
[19]J. J. Ramasco, J. M. López, and M. A. Rodríguez, Phys. Rev. Lett. **84**, 2199 (2000).
[20]M. A. Auger, L. Vazquez, O. Sanchez, M. Jergel, R. Cuerno, and M. Castro, J. Appl. Phys. **97**, 123528 (2005).
[21]M. A. Auger, L. Vazquez, R. Cuerno, M. Castro, M. Jergel, and O. Sanchez, Phys. Rev. B **73**, 045436 (2006).
[22]J. Aué and J. Th. M. De Hosson, Appl. Phys. Lett. **71**, 1347 (1997).
[23]M. Moseler, P. Gumbsch, C. Casiraghi, A. C. Ferrari, and J. Robertson, Science **309**, 1545 (2005).
[24]R. Q. Zhang, X. H. Xu, S. Y. Zhang, and G. Gehring, Phys. Rev. B **78**, 075419 (2008).
[25]M. Kilo, C. Argirusis, G. Borchardt, and R. Jackson, Phys. Chem. Chem. Phys. **5**, 2219 (2003).
[26]E. Vasco, C. Zaldo, and L. Vázquez, J. Phys. Condens. Matter **13**, L663 (2001).
[27]M. J. Aziz, Appl. Phys. A: Mater. Sci. Process. **93**, 579 (2008).
[28]S. Mráz and J. M. Schneider, J. Appl. Phys. **100**, 023503 (2006).